View Article Online / Journal Homepage / Table of Contents for this issue

Dalton Transactions

An international journal of inorganic chemistry

www.rsc.org/dalton

Number 22 | 14 June 2008 | Pages 2901–3016

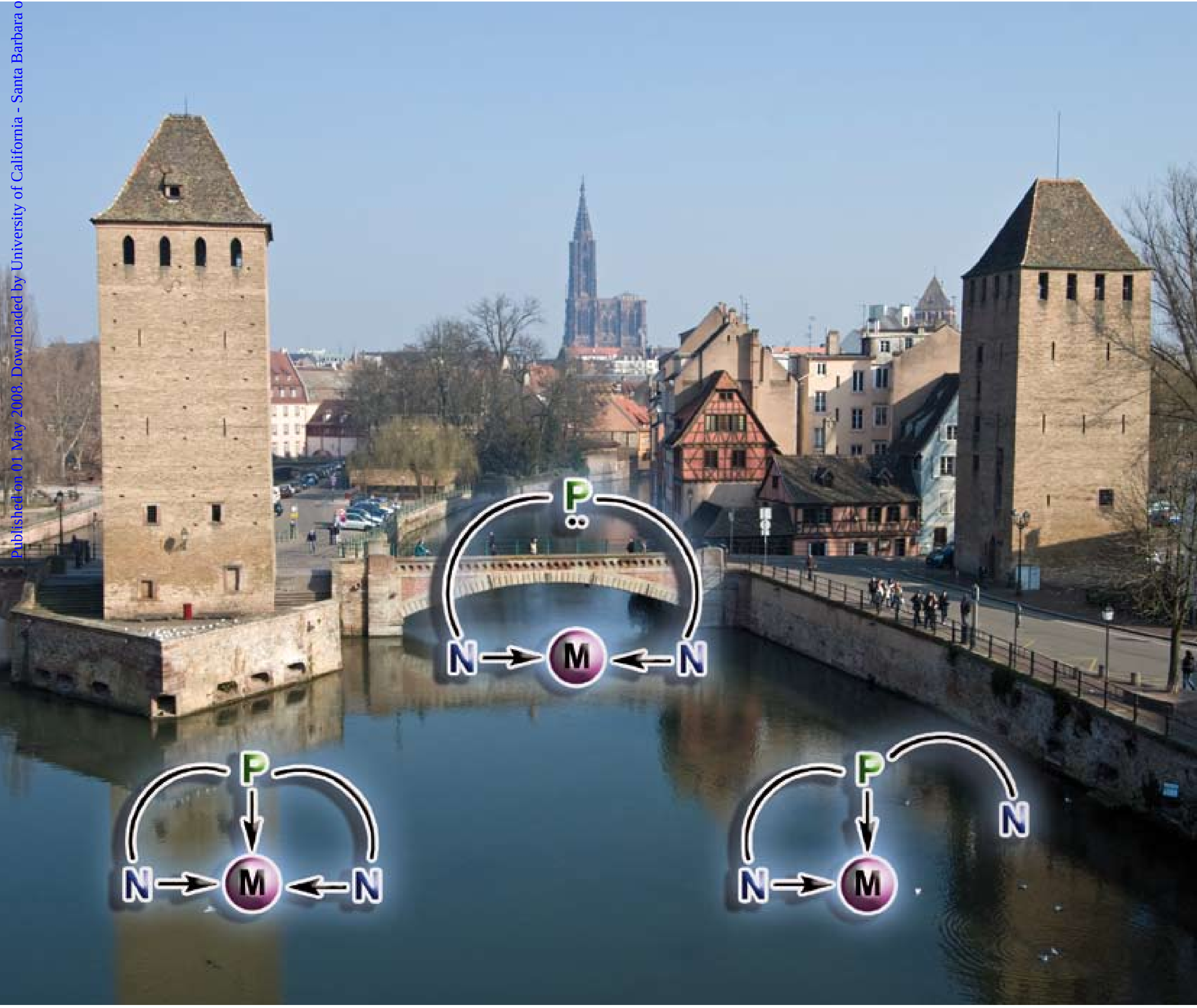

ISSN 1477-9226

RSC Publishing

HOT ARTICLE
Braunstein *et al.*
Nickel and iron complexes with N,P,N-type ligands

PERSPECTIVE
Bo and Maseras
QM/MM methods in inorganic chemistry

1477-9226(2008)22;1-5

Nickel and iron complexes with N,P,N-type ligands: synthesis, structure and catalytic oligomerization of ethylene†

Anthony Kermagoret, Falk Tomicki and Pierre Braunstein*

Received 4th February 2008, Accepted 20th March 2008
First published as an Advance Article on the web 1st May 2008
DOI: 10.1039/b802009d

The N,P,N-type ligands bis(2-picolyl)phenylphosphine (**1**), bis(4,5-dihydro-2-oxazolylmethyl)phenylphosphine (**2**), bis(4,4-dimethyl-2-oxazolylmethyl)phenylphosphine (**3**) and bis(2-picolyloxy)phenylphosphine (**4**) were used to synthesize the corresponding pentacoordinated Ni(II) complexes [Ni{bis(2-picolyl)phenylphosphine}Cl_2] (**6**), [Ni{bis(4,5-dihydro-2-oxazolylmethyl)phenylphosphine}Cl_2] (**7**), [Ni{bis(4,4-dimethyl-2-oxazolylmethyl)phenylphosphine}Cl_2] (**8**) and [Ni{bis(2-picolyloxy)phenylphosphine}Cl_2] (**9**), respectively. The hexacoordinated iron complexes [Fe{bis(2-picolyl)phenylphosphine}$_2$][$Cl_3FeOFeCl_3$] (**10**), [Fe{bis(4,5-dihydro-2-oxazolylmethyl)phenylphosphine}$_2$][$Cl_3FeOFeCl_3$] (**11**) and the tetracoordinated complex [Fe{bis(4,4-dimethyl-2-oxazolylmethyl)phenylphosphine}Cl_2] (abbreviated [$FeCl_2(NPN^{Me2}$-*N,N*)]) were prepared by reaction of $FeCl_2\cdot 4H_2O$ with ligands **1–3**, respectively. The crystal structures of the octahedral complexes **10** and **11**, determined by X-ray diffraction, showed that two tridentate ligands are facially coordinated to the metal centre with a *cis*-arrangement of the P atoms and the dianion (μ-oxo)bis[trichloroferrate(III)] compensates the doubly positive charge of the complex. The cyclic voltammograms of **10** and **11** showed two reversible redox couples attributed to the reduction of the dianion $(Fe_2OCl_6)^{2-}$ (−0.24 V for **10** and −0.20 V for **11** *vs.* SCE) and to the oxidation of the Fe(II) ion of the complex (0.67 V for **10** and 0.52 V for **11** *vs.* SCE). The cyclic voltammogram of [$FeCl_2(NPN^{Me2}$-*N,N*)] showed a reversible redox couple at −0.17 V *vs.* SCE assigned to the oxidation of the Fe(II) atom and an irreversible process at 0.65 V. The complexes **6**, **8–11** and [$FeCl_2(NPN^{Me2}$-*N,N*)] have been evaluated in the catalytic oligomerization of ethylene with $AlEtCl_2$ or MAO as cocatalyst. The nickel complex **6** proved to be the most active precatalyst in the series, with a turnover frequency (TOF) of $61\,800\ \mathrm{mol}_{C_2H_4}\ \mathrm{mol}_{Ni}^{-1}\ \mathrm{h}^{-1}$ with 10 equiv. of $AlEtCl_2$ and $12\,200\ \mathrm{mol}_{C_2H_4}\ \mathrm{mol}_{Ni}^{-1}\ \mathrm{h}^{-1}$ with 200 equiv. of MAO. Precatalysts **8** and **9** were the most selective in butenes, up to 90% with 6 equiv. of $AlEtCl_2$ and 89% with 2 equiv. of $AlEtCl_2$, respectively, and up to 92% butenes with 400 equiv. of MAO and 91% butenes with 200 equiv. MAO, respectively. The best selectivities for 1-butene were provided by **8** and $AlEtCl_2$ (up to 31% with 6 equiv.) and **9** with MAO (up to 72% with 200 equiv.). The iron complexes were not significantly active with $AlEtCl_2$ or MAO as cocatalyst.

Introduction

There is considerable current academic and industrial interest in catalytic ethylene oligomerization, in particular for the production of linear α-olefins in the C_4–C_{10} range whose demand is growing fast. The need for identifying and fine-tuning the parameters which influence the activity and selectivity of metal catalysts is generating much effort at the interface between ligand design, coordination/organometallic chemistry and homogeneous catalysis.[1] We reported recently the synthesis of various mono- and dinuclear nickel complexes bearing five-, six-, or seven-membered P,N-chelating ligands in which the P donor function was of the phosphine, phosphonite or phosphinite-type and the N donor was part of a pyridine or oxazoline heterocycle (Scheme 1).[1e,2]

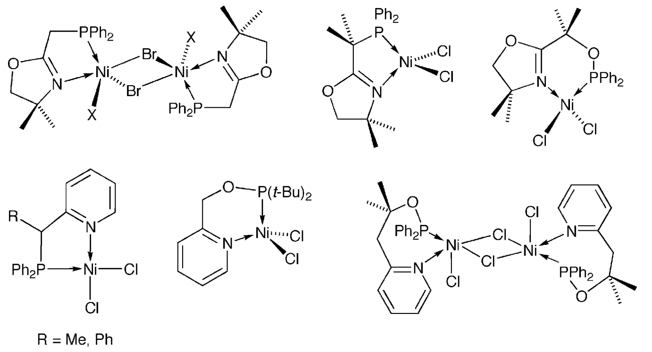

Scheme 1 Some Ni(II) complexes with P,N-type ligands.

The coordination geometry about the metal was found to strongly depend on the ligand substituents and ranged from square-planar or tetrahedral for mononuclear complexes to square-pyramidal or trigonal bipyramidal for dinuclear complexes.

Laboratoire de Chimie de Coordination, Institut de Chimie (UMR 7177 CNRS), Université Louis Pasteur, 4 rue Blaise Pascal, F-67070, Strasbourg Cédex, France. E-mail: braunstein@chimie.u-strasbg.fr

† CCDC reference numbers 676912 and 676913. For crystallographic data in CIF or other electronic format see DOI: 10.1039/b802009d

In the presence of even small amounts of $AlEtCl_2$ or MAO as cocatalyst, these Ni(II) complexes turned out to be highly active and selective precatalysts for ethylene dimerization.[1e,2]

Investigations with related tridentate N,P,N-type ligands toward the formation of new oligomerization catalysts led to the synthesis of the pentacoordinated mononuclear nickel complex $[NiCl_2(NOPON^{Me2}\text{-}N,P,N)]$ ($NOPON^{Me2}$ = bis(4,4-dimethyl-2-oxazolyldimethylmethoxy)phenylphosphine, Scheme 2), which is an effective precatalyst leading to selectivities in C_4 olefins higher than 90% when activated with $AlEtCl_2$.[3]

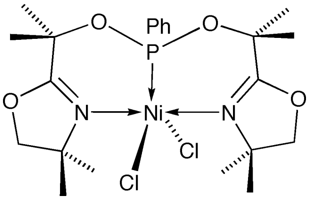

Scheme 2 The complex $[NiCl_2(NOPON^{Me2}\text{-}N,P,N)]$.

The use of the $NOPON^{Me2}$ ligand was extended to the formation of the new Co(II) complex $[CoCl_2(NOPON^{Me2}\text{-}P,N)]$ (Scheme 3) which also catalyzes ethylene oligomerization in the presence of $AlEtCl_2$ as a cocatalyst.[4] In contrast to the pentacoordination observed in $[NiCl_2(NOPON^{Me2}\text{-}N,P,N)]$, $[CoCl_2(NOPON^{Me2}\text{-}P,N)]$ is tetracoordinated and displays bidentate P,N-coordination of the ligand with one pendant oxazoline arm. A comparative study of the behaviour of related phosphonite and phosphine N,P,N ligands toward Co(II) precursors led to the synthesis of the new complex $[CoCl_2(NPN^{Me2}\text{-}N,N)]$ (NPN^{Me2} = bis(4,4-dimethyl-2-oxazolylmethyl)phenylphosphine (**3**)) (Scheme 3). Its structural determination revealed an unexpected N,N-chelation mode of the ligand and the lack of phosphorus coordination contrasted with the situation in $[CoCl_2(NOPON^{Me2}\text{-}P,N)]$.[4]

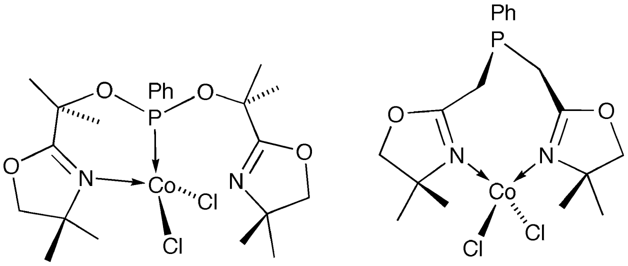

Scheme 3 The complexes $[CoCl_2(NOPON^{Me2}\text{-}P,N)]$ and $[CoCl_2(NPN^{Me2}\text{-}N,N)]$.

Because of the different P,N- and N,N-coordination modes observed in the Co(II) complexes $[CoCl_2(NOPON^{Me2}\text{-}P,N)]$ and $[CoCl_2(NPN^{Me2}\text{-}N,N)]$, respectively, we wished to compare the structure of the products obtained from $NOPON^{Me2}$ or NPN^{Me2} and different Pd(II) precursors. The nature of the counteranion was found to play a crucial role on the ligand coordination mode:[4,5] halides led to a P,N-coordination mode of the ligands $NOPON^{Me2}$ and NPN^{Me2}, whereas non-coordinating anions, such as BF_4^-, resulted in N,P,N-coordination (Scheme 4).

During attempts to synthesize iron complexes with the $NOPON^{Me2}$ ligand by its reaction with anhydrous $FeCl_3$, cleavage of the P–O bond was observed and the dinuclear complex $[FeCl_2(4,4\text{-dimethyl-2-oxazolyldimethylmethanolate})]_2$ was isolated which contains the N,O ligand bonded in a μ-$\eta^1(O)$:$\eta^2(N,O)$ manner (the complex is abbreviated as $[Fe^{III}\{\mu\text{-}\eta^1(O)\text{:}\eta^2(N,O)\}Cl_2]_2$) (Scheme 5).[3] In contrast, the reaction between $FeCl_2\cdot4H_2O$ and the ligand NPN^{Me2} yielded the complex $[FeCl_2(NPN^{Me2}\text{-}N,N)]$ in which the ligand displays a N,N coordination mode (Scheme 5), similar to that in $[CoCl_2(NPN^{Me2}\text{-}N,N)]$.[4]

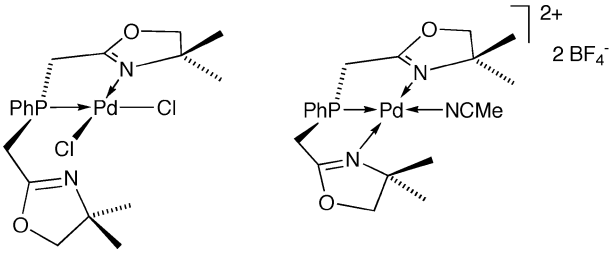

Scheme 4 The complexes $[PdCl_2(NPN^{Me2}\text{-}P,N)]$ and $[Pd(NPN^{Me2}\text{-}N,P,N)(NCMe)](BF_4)_2$.

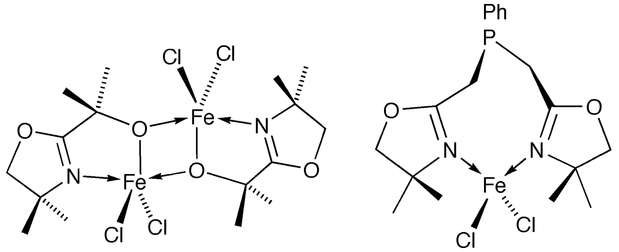

Scheme 5 The complexes $[Fe^{III}\{\mu\text{-}\eta^1(O)\text{:}\eta^2(N,O)\}Cl_2]_2$ and $[Fe^{II}Cl_2(NPN^{Me2}\text{-}N,N)]$.

This diversity of results prompted us to study further the coordination behaviour of tridentate N,P,N-type ligands with iron and nickel complexes. Only a few nickel complexes coordinated by N,P,N ligands have been synthesized,[6] although they might have promising applications in the catalytic oligomerization of ethylene.

Results and discussion

Synthesis of the ligands

The phosphino-pyridine ligand **1** was prepared according to the literature[7] but the yield can be increased if 2-[(trimethylsilyl)methyl]pyridine is isolated by distillation before $PPhCl_2$ is added [eqn (1)]. The pure ligand was obtained in yields up to 68% and it has been characterized by ^1H, $^{31}P\{^1H\}$ and $^{13}C\{^1H\}$ NMR spectroscopic methods.

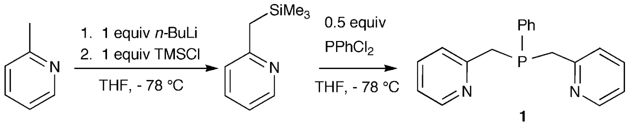

1

(1)

The phosphino-oxazoline ligands **2** and **3** were prepared as descibed by deprotonation of the corresponding oxazoline precursor followed first by the addition of chlorotrimethylsilane and then addition of 0.5 equiv. of $PPhCl_2$ at −78 °C [eqn (2)].[4,8]

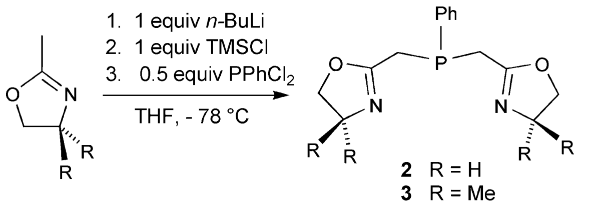

(2)

Owing to the presence of the prochiral P centre, the CH$_2$ protons in α position to the phosphorus atom of ligand **2** display an ABMX spin system (A = B = M = H, X = P)[8] and the signals of the PCH$_2$ protons of **1** and **3**[4] correspond to ABX spin systems (A = B = H, X = P).

The sensitivity of phosphonites to the presence of HCl[3] prevents an efficient synthesis of **4** by direct reaction of PPhCl$_2$ with (pyridine-2-yl)methanol, which leads in addition to **4** to (pyridin-2-yl)methyl hydrogen phenylphosphonate **5** and 2-(chloromethyl)pyridine by-products despite the presence of NEt$_3$ [eqn (3)].

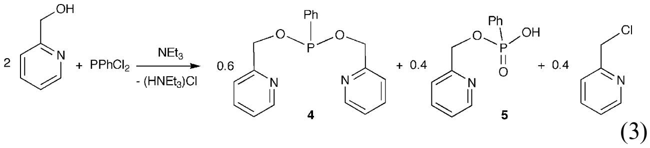

(3)

However, the reaction of two equiv. of pyridine alcoholate with one equiv. of PPhCl$_2$ at −78 °C in THF yielded the desired tridentate pyridine-phosphonite ligand **4** [eqn (4)]. Its ^{1}H NMR spectrum contains an ABX spin system (A = B = H, X = P) for the CH$_2$ protons.

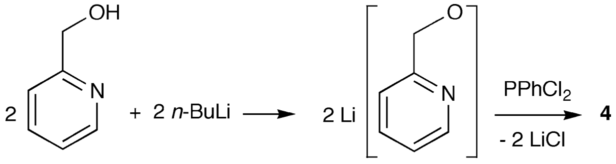

(4)

Synthesis of the nickel complexes

The Ni(II) bis(2-picolyl)phenylphosphine complex **6** and the bis(2-oxazolylmethyl) phenylphosphine complexes **7** and **8** were prepared in MeOH by reaction between equimolar amounts of NiCl$_2$ with the N,P,N ligands **1–3**, respectively, and isolated in yields of 96%, 61% and 77%, respectively.

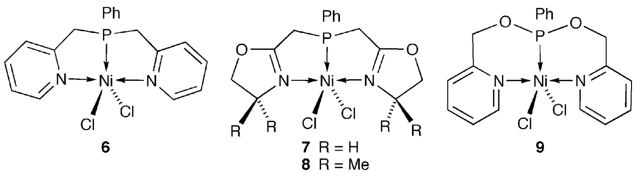

Complex **9** was obtained by stirring one equiv. of ligand with one equiv. of [NiCl$_2$(DME)] (DME = 1,2-dimethoxyethane) in CH$_2$Cl$_2$ at room temperature. This Ni(II) precursor was preferred over NiCl$_2$·6H$_2$O[9] because of its better solubility in CH$_2$Cl$_2$ and methanol should be avoided as a solvent with ligands containing a P–OR bond.[2] Coordination of the ligand to the metal centre was confirmed in IR spectroscopy by the strong absorption corresponding to the ν(C=N) vibrations at 1600, 1658, 1636 and 1603 cm^{-1} for **6–9**, respectively. The IR spectra of **6–9** did not show the presence of uncoordinated pyridine or oxazoline functions and this suggested a tridentate behaviour for ligands **1–4**, similar to that found in [NiCl$_2$(NOPON$^{\mathrm{Me2}}$-*N,P,N*)].[3] The strong IR band at 1270 cm^{-1} for **7** shifts to 1320 cm^{-1} for the methyl substituted derivative **8**. The nickel complexes **6–9** are paramagnetic in solution and their magnetic moments, determined in CD$_2$Cl$_2$ by the Evans method,[10–13] were 3.1, 2.7, 2.8 and 2.7 μ_B, respectively. These values are in the range found for Ni(II) complexes coordinated by P,N type ligands.[3,13–16] Complexes **6–9** were characterized by IR spectroscopy and elemental analysis and their green colour in the solid state is comparable with that of related five-coordinated complexes.[3] It is noteworthy that bidentate P,N chelates, such as Ph$_2$PCH$_2$ox where ox represents the oxazoline featured in **2** were recently shown to give rise to the formation of interconvertible mono- and tetranuclear Ni(II) complexes.[17]

Synthesis of the iron complexes

In scheme 6 are summarized the syntheses of the Fe(II) complexes **10**, **11** and [FeCl$_2$(NPN$^{\mathrm{Me2}}$-*N,N*)],[4] which were obtained by reaction of one equiv. of FeCl$_2$·4H$_2$O with the ligands **1–3**, respectively.

During their synthesis, complexes **10** and **11** precipitated instantaneously from CH$_2$Cl$_2$ and, after work-up, they were isolated as red powders in 62% and 58% yield, respectively. The IR spectrum of complex **10** was similar to that of the corresponding Ni complex **6**. The strong IR band for the ν(C=N) vibration of **11** at 1639 cm^{-1} is shifted towards lower wavenumbers compared to that of its corresponding nickel complex **7** (1658 cm^{-1}). Slow diffusion of heptane into a CH$_2$Cl$_2$–MeCN (1 : 1) solution of the complexes **10** and **11** afforded crystals suitable for X-ray diffraction. ORTEP views of their crystal structures are presented in Fig. 1 and 2 and selected bond distances and angles are given in Tables 1 and 2, respectively.

The X-ray structural analyses established the *fac*-coordination of each tridentate ligand and the mutual *cis*-position of the P donors in these octahedral complexes. Interestingly, the reaction of **2** with [RuCl$_2$(DMSO)$_4$] or [RuCl$_2$(PPh$_3$)$_3$] has previously led to the formation of the dichloro complexes **12** and **13**, respectively, in which there is only one tridentate N,P,N ligand coordinated to the

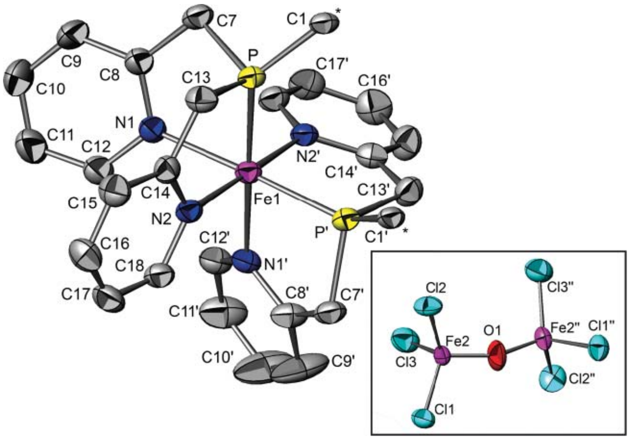

Fig. 1 ORTEP view of the structure of **10** in **10**·0.5CH$_2$Cl$_2$ with thermal ellipsoids drawn at the 50% probability level, symmetry operator for the generation equivalent position: −*x* + 1/2, −*y* + 1/2, *z* (′) and −*x* + 1/2, −*y* + 3/2, *z* (″).

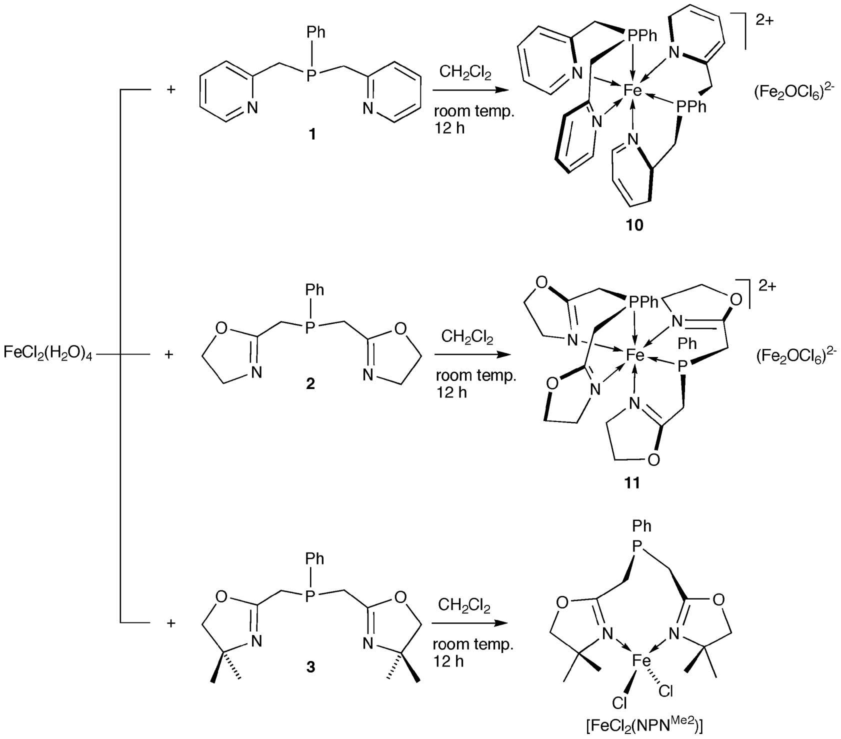

Scheme 6 Comparative synthesis of the iron complexes **10**, **11** and [FeCl$_2$(NPN^{Me2}-*N,N*)].

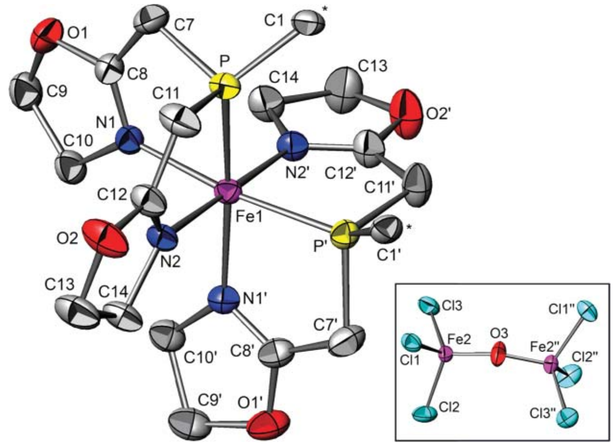

Fig. 2 ORTEP view of the structure of **11** in **11**·4MeCN with thermal ellipsoids drawn at the 50% probability level, symmetry operator for the generation equivalent position: $-x, y, -z + 1/2$ (′) and $-x + 1, y, -z + 1/2$ (″).

metal centre, also in a *fac*-coordination mode, and their octahedral geometry was achieved by further coordination of one molecule of DMSO or PPh$_3$, respectively.[8,18]

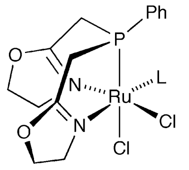

12 L = DMSO
13 L = PPh$_3$

Table 1 Selected bond distances (Å) and angles (°) in **10**·0.5CH$_2$Cl$_2$[a]

Fe1–P	2.165(2)	C7–P	1.831(6)
Fe1–N1	2.097(4)	P–C13	1.823(6)
Fe1–N2	2.022(4)	C13–C14	1.506(8)
N1–C8	1.355(7)	C14–N2	1.356(7)
C8–C7	1.506(8)	Fe2–O1	1.754(2)
P–Fe1–N1	81.5(2)	N1–Fe1–P′	177.5(2)
P–Fe1–N1′	177.5(2)	N2–Fe1–N1′	96.7(2)
P–Fe1–N2	85.6(2)	N2–Fe1–N2′	176.9(2)
P–Fe1–N2′	96.4(2)	N2–Fe1–P′	96.4(2)
P–Fe1–P′	99.33(9)	N1′–Fe1–N2′	81.3(2)
N1–Fe1–N1′	97.9(3)	N1′–Fe1–P′	81.5(2)
N1–Fe1–N2	81.3(2)	N2′–Fe1–P′	85.6(2)
N1–Fe1–N2′	96.7(2)	Fe2–O1–Fe2″	154.1(5)

[a] Symmetry operator for the generation equivalent position: $-x + 1/2, -y + 1/2, z$ (′) and $-x + 1/2, -y + 3/2, z$ (″).

Table 2 Selected bond distances (Å) and angles (°) in **11**·4MeCN [a]

Fe1–P	2.1842(6)	C7–P	1.841(2)
Fe1–N1	2.042(2)	P–C11	1.836(2)
Fe1–N2	1.989(2)	C11–C12	1.474(3)
N1–C8	1.276(3)	C12–N2	1.274(3)
C8–C7	1.486(3)	Fe2–O3	1.7600(5)
P–Fe1–N1	82.95(5)	N1–Fe1–P′	170.62(5)
P–Fe1–N1′	170.61(5)	N2–Fe1–N1′	88.44(7)
P–Fe1–N2	82.40(5)	N2–Fe1–N2′	179.0(1)
P–Fe1–N2′	98.25(5)	N2–Fe1–P′	98.25(5)
P–Fe1–P′	96.26(3)	N1′–Fe1–N2′	90.92(7)
N1–Fe1–N1′	99.34(9)	N1′–Fe1–P′	82.95(5)
N1–Fe1–N2	88.44(7)	N2′–Fe1–P′	82.40(5)
N1–Fe1–N2′	90.92(7)	Fe2–O3–Fe2″	162.0(2)

[a] Symmetry operator for the generation equivalent position: $-x, y, -z + 1/2$ (′) and $-x + 1, y, -z + 1/2$ (″).

Complexes **10** and **11** adopt a distorted octahedral geometry as shown by the values of the P–Fe1–N1′ and N2–Fe1–N2′ angles (177.5(2) and 176.9(2)°, respectively, for **10** and 170.61(5) and 179.0(1)°, respectively, for **11** (Tables 1 and 2). The phosphorus atoms are coordinated to the Fe(II) ion *trans* to a nitrogen atom and the dications have a C_2 symmetry axis passing through the metal centre. For **11**, the Fe1–N1 bond distance (2.042(2) Å), slightly longer than Fe1–N2 (1.989(2) Å), results from the *trans* influence of the phosphorus atom on N1. This is also noted in complex **10** with the slightly longer Fe1–N1 distance (2.097(4) Å) compared to Fe1–N2 (2.022(4) Å).

The doubly positive charge of the metal complex in **10** or **11** is compensated by the dianion (μ-oxo)bis[trichloroferrate(III)] $(Fe_2OCl_6)^{2-}$ which results from the partial oxidation of the Fe(II) precursor.[19–22] Complexes where a Fe(II) centre is coordinated by two tridentate ligands have been described with a $(FeCl_4)^{2-}$ counter ion.[23–27] Since its first description in 1978, this ferric dianion has been studied for its magnetic or structural properties and its tetraalkylammonium derivatives $(R_4N)_2(Fe_2OCl_6)$ are convenient starting materials for the synthesis of polynuclear iron complexes.[28–32] Iron complexes containing $(Fe_2OCl_6)^{2-}$ have been reported and formation of this dianion could occur *via* an intermediate Fe(II) anion which rapidly autoxidizes.[19–22,32–36] The overall stoichiometry of three iron atoms for two ligands in complexes **10** and **11** suggests the loss of one third of the ligands **1** and **2**.

Despite the similar Fe2–O distances in the dianion present for **10** and **11** (1.754(2) and 1.7600(5) Å, respectively), the Fe2–O1–Fe2″ bond angle in **10** (154.1(5)°) is smaller than the corresponding Fe2–O3–Fe2″ angle in **11** (162.0(2)°). According to the literature, the Fe–O distance in the dianion $(Fe_2OCl_6)^{2-}$ is generally found around 1.76 Å but the value of the Fe–O–Fe angle varies between 147.7 and 180.0°.[30,35]

The white complex $[FeCl_2(NPN^{Me2}\text{-}N,N)]$ was obtained in 87% yield[4] and its magnetic moment of 4.2 μ_B has now been determined in CD_2Cl_2 by the Evans method.[10–13] This value is slightly lower than expected for Fe(II) high spin complexes.[37,38] Its crystal structure showed a distorted tetrahedral geometry with the N,N-coordination of ligand **3** without the expected coordination of the phosphorus to the iron centre.[4] The N,N-chelating behaviour of **3** in $[FeCl_2(NPN^{Me2}\text{-}N,N)]$ compared to the N,P,N-tridentate behaviour of **2** in **11** appears to be related to the steric effects generated by the presence of methyl substituents on the oxazoline ring. Depending on the nature of the counteranion present, ligand **3** has been found to adopt either P,N or N,P,N coordination modes in Pd(II) complexes and phosphorus coordination to the metal centre was confirmed by $^{31}P\{^1H\}$ NMR spectroscopy.[4] The role of the counter-anion on the coordination mode of ligand **2** has also been studied with cationic Ru(II)–benzene complexes and P,N coordination was observed with monocationic complexes and N,P,N coordination with dicationic complexes.[8] The ease of conversion between the different coordination modes of **2** and **3** is consistent with their hemilabile properties.[4,39]

The crystal structure of **10** suggested that ligands **1** and **2** have similar coordination behaviours despite the different nature of their heterocyclic nitrogen donor atom. It will be interesting to examine whether the addition of substituents on the pyridine function, to increase the steric component, could also lead to the formation of metal complexes with a N,N coordination of the ligand.

Electrochemistry

The complexes **10**, **11** and $[FeCl_2(NPN^{Me2}\text{-}N,N)]$ have been studied by cyclic voltammetry (Fig. 3 and 4). The cyclic voltammograms of **10** and **11** (Fig. 3) showed two reversible redox couples attributed respectively to the reduction of the dianion $(Fe_2OCl_6)^{2-}$ (−0.24 V for **10** and −0.20 V for **11** *vs.* SCE) and to the oxidation of the Fe(II) centre of the complex (0.67 V for **10** and 0.52 V for **11** *vs.* SCE). Coordinated by pyridine functions, the more electron-rich **10** has a redox potential for the Fe(II) centre shifted to more positive values compared to **11** and this indicates a slightly higher stability of Fe(II) in **10** than in **11**. However, compared to Fe(II) complexes coordinated by two N,N,N-tridentate ligands containing pyridine functions and with redox potentials between 0.78 and 1.06 V *vs.* SCE, the redox potential of **10** is at less positive values.[40,41]

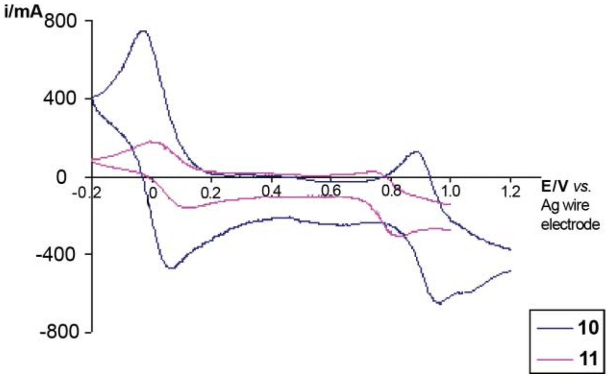

Fig. 3 Cyclic voltammograms of **10** and **11** in anhydrous MeCN (0.1 M $N(n\text{-}Bu)_4PF_6$) at a scan rate of 100 mV s^{-1}.

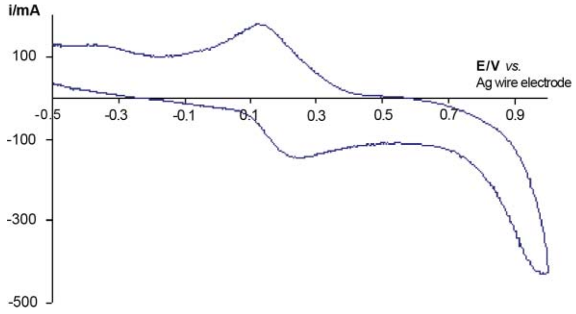

Fig. 4 Cyclic voltammogram of $[FeCl_2(NPN^{Me2}\text{-}N,N)]$ in anhydrous MeCN (0.1 M $N(n\text{-}Bu)_4PF_6$) at a scan rate of 100 mV s^{-1}.

The cyclic voltammogram of $[FeCl_2(NPN^{Me2}\text{-}N,N)]$ showed a reversible redox couple at −0.17 V *vs.* SCE attributed to the oxidation of the Fe(II) centre and an irreversible process at 0.65 V (Fig. 4). This potential is slightly more negative than in Fe(II) complexes coordinated by α-diimine ligands.[42]

Catalytic oligomerization of ethylene

The complexes **6**, **8–11** and $[FeCl_2(NPN^{Me2}\text{-}N,N)]$ have been evaluated in the catalytic oligomerization of ethylene with different amounts of $AlEtCl_2$ or MAO as cocatalyst. The complex [$NiCl_2\{P(n\text{-}Bu)_3\}_2$], which is a typical oligomerization precatalyst,[43] was used as a reference. The Ni complexes **6**, **8** and **9** were active when 2, 4, 6 or 10 equiv. of $AlEtCl_2$ (Table 3) or 200 or 400 equiv. of MAO (Table 4) were used as cocatalyst (Fig. 5–9). In contrast to **6**, complexes **8** and **9** did not have significant catalytic activities with 100 equiv. of MAO. Complex **6** was the most active, with a turnover frequency (TOF) of 61 800 $mol_{C_2H_4}\ mol_{Ni}^{-1}\ h^{-1}$ with 10 equiv. of $AlEtCl_2$ (Fig. 5) and of 12 200 $mol_{C_2H_4}\ mol_{Ni}^{-1}\ h^{-1}$ with 200 equiv. of MAO (Fig. 7). With $AlEtCl_2$ as cocatalyst, **8** showed the best selectivities for butenes (up to 90% with 6 equiv. of $AlEtCl_2$ and up to 31% 1-butene) whereas with MAO, **9** was the most selective, leading to up to 92% butenes with 400 equiv. of MAO and up to 72% 1-butene with 200 equiv. of MAO. Similarly to Ni(II) complexes with P,N-type ligands, complexes **6** and **9** coordinated by pyridine functions afforded with $AlEtCl_2$ or MAO as cocatalyst better activities than the oxazoline-based systems **8** and [$NiCl_2(NOPON^{Me2}\text{-}N,P,N)$], respectively.[3]

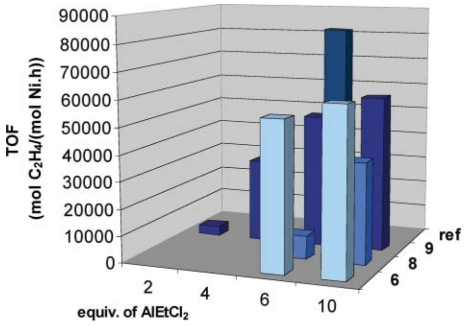

Fig. 5 Catalytic activities of the complexes **6**, **8** and **9** in the oligomerization of ethylene using $AlEtCl_2$ as cocatalyst, Ref: [$NiCl_2\{P(n\text{-}Bu)_3\}_2$].

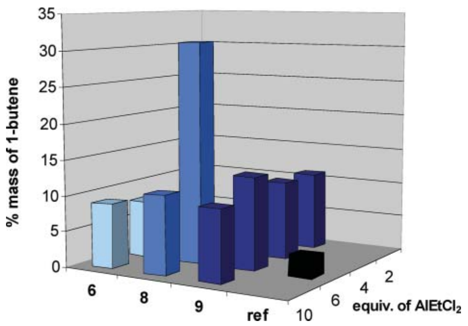

Fig. 6 Selectivity of the complexes **6**, **8** and **9** for 1-butene using $AlEtCl_2$ as cocatalyst, Ref: [$NiCl_2\{P(n\text{-}Bu)_3\}_2$].

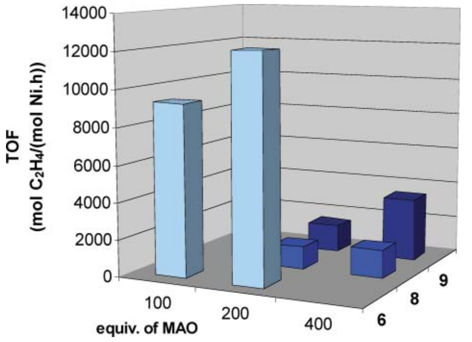

Fig. 7 Catalytic activities of the complexes **6**, **8** and **9** in the oligomerization of ethylene using MAO as cocatalyst.

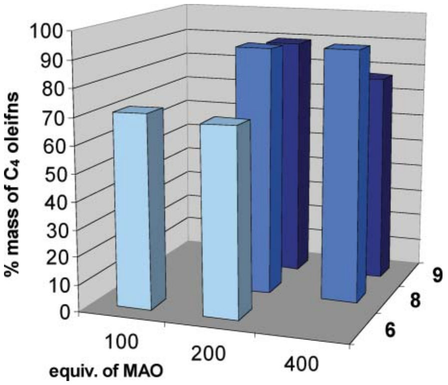

Fig. 8 Selectivity of the complexes **6**, **8** and **9** for C_4 compounds using MAO as cocatalyst (1-butene and 2-butene).

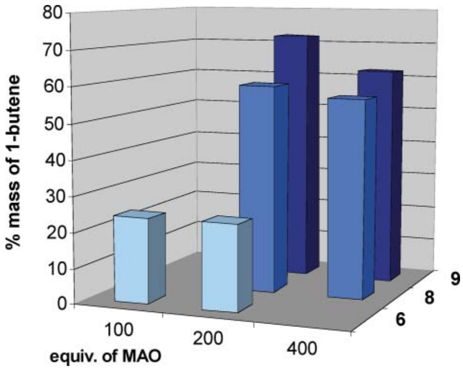

Fig. 9 Selectivity of the complexes **6**, **8** and **9** for 1-butene using MAO as cocatalyst.

The nature of the cocatalyst has an impact on the catalytic results: MAO leads to systems less active but more selective in 1-butene and in C_4 olefins than $AlEtCl_2$. Increasing the amount of cocatalyst makes the system more active but less selective in C_4 olefins and in 1-butene. As shown by **6** with $AlEtCl_2$ as cocatalyst, very active systems favored the isomerization of 1-butene in 2-butene (selectivity in 1-butene less than 9%, Fig. 6) and the reinsertion of 1-butene and 2-butene to form C_6 oligomers (selectivity in C_6 oligomers up to 43%, Table 3).

A comparison of the catalytic results of **6** and **9** with $AlEtCl_2$ as cocatalyst with those obtained with **14** and **15** indicates that precatalysts coordinated by a P,N chelate lead to slightly higher activities than those coordinated by a N,P,N tridentate ligand.[2] However, this does not significantly affect the selectivities in C_4 olefins and in 1-butene. With MAO as cocatalyst, **15** was more active but significantly less selective in 1-butene than **9**, despite similar catalytic results observed for **6** and **14**.[2]

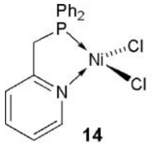

14

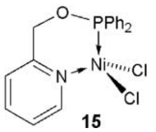

15

Some tetrahedral iron(II) complexes have shown good activities in oligomerization and polymerization of ethylene[44,45] and it was therefore interesting to test [$FeCl_2(NPN^{Me2}\text{-}N,N)$] with different

Table 3 Comparative catalytic data for complexes **6**, **8** and **9** in the oligomerization of ethylene with $AlEtCl_2$ as cocatalyst[a]

		Selectivity (mass%)						
	$AlEtCl_2$ (equiv.)	C_4	C_6	C_8	Productivity/$g_{C_2H_4}$ g_{Ni}^{-1} h^{-1}	TOF/$mol_{C_2H_4}$ mol_{Ni}^{-1} h^{-1}	α-Olefin (C_4)[b] (%)	k_α[c]
6	6	53	43	4	26 400	55 600	8	0.57
6	10	54	42	4	29 500	61 800	9	0.55
8	6	90	10	<1	4 200	8 800	31	<0.10
8	10	76	23	1	18 000	37 700	11	0.20
9	2	89	11	<1	1 600	3 400	11	<0.10
9	4	77	21	2	14 900	31 300	11	0.18
9	6	53	41	6	23 800	49 900	13	0.51
9	10	53	43	4	27 800	58 200	8	0.57
Ref[d]	6	60	35	5	38 800	81 400	3	0.40

[a] Conditions: $T = 30$ °C, 10 bar of C_2H_4, 35 min, 4×10^{-5} mol Ni complex; solvent 12 or 10 mL chlorobenzene and 3 or 5 mL of cocatalyst toluene solution for 6 or 10 equiv. of $AlEtCl_2$, respectively (total volume 15 mL). [b] Within the C_4 fraction. [c] k_α = hexenes (mol)/butenes (mol). [d] Ref = $[NiCl_2\{P(n\text{-}Bu)_3\}_2]$.

Table 4 Comparative catalytic data for complexes **6**, **8** and **9** in the oligomerization of ethylene with MAO as cocatalyst[a,b]

		Selectivity (mass%)						
	MAO (equiv.)	C_4	C_6	C_8	Productivity/$g_{C_2H_4}$ g_{Ni}^{-1} h^{-1}	TOF/$mol_{C_2H_4}$ mol_{Ni}^{-1} h^{-1}	α-Olefin (C_4)[c] (%)	k_α[d]
6	100	71	26	3	3900	9300	24	0.24
6	200	69	25	6	5800	12200	24	0.24
8	200	91	8	<1	500	1200	56	<0.10
8	400	92	7	<1	700	1500	59	<0.10
9	200	91	8	<1	700	1500	72	<0.10
9	400	77	20	3	1600	3400	62	0.17

[a] Conditions: $T = 30$ °C, 10 bar of C_2H_4, 35 min, 4×10^{-5} mol Ni complex; complex dissolved in 10 mL chlorobenzene to which 4, 8 or 16 mL of cocatalyst solution in toluene is added for 100, 200 or 400 equiv. of MAO, respectively. [b] Traces of C_{10} oligomers were detected when using 400 equiv. of MAO. [c] Within the C_4 fraction. [d] k_α = hexenes (mol)/butenes (mol).

cocatalysts. However, with 200 equiv. of MAO or 6 equiv. of $AlEtCl_2$, $[FeCl_2(NPN^{Me2}\text{-}N,N)]$ was poorly active and only traces of butenes were detected by gas chromatography. The hexacoordinated mononuclear iron complexes **10** and **11** showed no activity with MAO or $AlEtCl_2$ as cocatalyst, probably because of the saturated coordination sphere of the iron centre which inhibits ethylene coordination to the metal centre. Similarly, iron complexes containing two C,N,C pincer ligands were also found inactive.[46,47]

Conclusion

The phosphino-pyridine **1**[7] and the phosphino-oxazoline ligands **2**[8] and **3**[4] and ligand **4**, synthesized by reaction of $PPhCl_2$ with 2 equiv. of its corresponding pyridine alcoholate at low temperature, were used to prepare the nickel complexes **6–9** in good yields by reaction with $NiCl_2$ in methanol or $[NiCl_2(DME)]$ in CH_2Cl_2. The IR spectra of **6–9** suggested the coordination of the two nitrogen atoms of the tridentate ligands **1–4**. Ligands **1–3** were also used for the preparation of the iron complexes **10** and **11** in which the dicationic Fe(II) centre is hexacoordinated and of the tetrahedral Fe(II) complex $[FeCl_2(NPN^{Me2}\text{-}N,N)]$.[4] The crystal structures of **10** and **11** also established the formation of the dianion (μ-oxo)bis[trichloroferrate(III)] to compensate the doubly positive charge. Whereas the cyclic voltammograms of **10** and **11** showed two reversible redox couples for the reduction of the dianion $(Fe_2OCl_6)^{2-}$ and the oxidation of the Fe(II) ion, that of $[FeCl_2(NPN^{Me2}\text{-}N,N)]$ showed a reversible redox couple (−0.17 mV *vs.* SCE) for the oxidation of the Fe(II) centre and an irreversible process (0.65 mV).

Complex **6** is the most active in ethylene oligomerization within the series, with a TOF of 61 800 $mol_{C_2H_4}$ mol_{Ni}^{-1} h^{-1} in the presence of 10 equiv. of $AlEtCl_2$ as cocatalyst and of 12 200 $mol_{C_2H_4}$ mol_{Ni}^{-1} h^{-1} with 200 equiv. of MAO. Precatalysts **8** and **9** were the most selective in butenes, up to 90% with 6 equiv. of $AlEtCl_2$ and 89% with 2 equiv. of $AlEtCl_2$, respectively, and up to 92% butenes with 400 equiv. of MAO and 91% butenes with 200 equiv. MAO, respectively. The more active systems favored the isomerization of 1-butene and the reinsertion of C_4 olefins to form C_6 oligomers. In all cases, the catalytic activity increased when more cocatalyst was used and $AlEtCl_2$ led to more active but less selective systems than MAO. The use of tridentate N,P,N ligands instead of bidentate P,N chelates resulted in slightly less active catalysts but similarly selective in C_4 olefins and 1-butene with $AlEtCl_2$ as cocatalyst. The iron complexes **10**, **11** and $[FeCl_2(NPN^{Me2}\text{-}N,N)]$ did not show significant activities in ethylene oligomerization, either with $AlEtCl_2$ or MAO as cocatalyst.

Experimental section

General considerations

All reactions were performed under purified nitrogen. Solvents were purified and dried under nitrogen by conventional methods. The ^1H NMR spectra were recorded at 300 MHz, $^{31}P\{^1H\}$ NMR spectra were recorded at 121.5 MHz, and $^{13}C\{^1H\}$ NMR spectra were recorded at 75.5 MHz on a FT Bruker AC300 instrument. IR spectra in the range of 4000–400 cm^{-1} were recorded on a Bruker IFS28FT. Gas chromatographic analyses were performed on a Thermoquest GC8000 Top Series gas chromatograph using a HP Pona column (50 m, 0.2 mm diameter, 0.5 µm film thickness). Magnetic moments were determined by the Evans method in CD_2Cl_2 using a solution of CH_3NO_2 in CD_2Cl_2 (20 : 80, v/v) as reference.[9–13] Mass spectra were recorded with a Bruker Daltonics microTOF (ESI; positive mode; capillary voltage: 4.8 kV; nebulizer pressure: 0.2 bar; desolvation temperature: 180 °C; desolvation gas flow rate: 4.5 L min^{-1}). Ligands **2**[8] and **3**,[4] and the complexes [$NiCl_2$(DME)][2] and [$FeCl_2$(NPN^{Me2}-*N*,*N*)][4] have been synthesized according to the literature.

Syntheses

Synthesis of bis(2-picolyl)phenylphosphine 1[7]. A *n*-BuLi solution (96.0 mmol, 1.6 M in hexane) was added dropwise to a degassed solution of 2-picoline (8.94 g, 96.0 mmol) in 100 mL of THF at −78 °C. After complete deprotonation, the red anion precipitated and after further stirring for 1 h at −78 °C, degassed chlorotrimethylsilane (10.43 g, 96.0 mmol) was added dropwise to the solution. The brown mixture was allowed to reach room temperature overnight and the THF was evaporated under reduced pressure. The residue was distilled at 120 °C and 12 mbar to obtain the pure, liquid 2-[(trimethylsilyl)methyl]pyridine (Yield: 6.61 g, 40.0 mmol, 42%). ^{1}H NMR (300 MHz, $CDCl_3$): δ 0.00 (s, 9H, $SiCH_3$), 2.32 (s, 2H, $SiCH_2$), 6.93 (t, $^2J_{H\text{-}H}$ = 7.65 Hz, 2H, aromatic H), 7.45 (td, 1H, $^2J_{H\text{-}H}$ = 1.85 Hz, $^2J_{H\text{-}H}$ = 7.65 Hz, aromatic H), 8.39 (d, 1H, $^3J_{H\text{-}H}$ = 4.17, CHCN). ^{13}C{^{1}H} NMR ($CDCl_3$, 75.5 MHz): δ −1.7 (s, $SiCH_3$), 30.2 (s, $SiCH_2$), 119.0 (s, C of pyridyl), 122.1 (s, C of pyridyl), 135.7 (s, C of pyridyl), 148.9 (s, C of pyridyl), 161.3 (s, C of pyridyl).

Pure picolyltrimethylsilane (6.61 g, 40.0 mmol) was dissolved in a mixture of 50 mL THF and 50 mL diethyl ether cooled down to −78 °C and $PPhCl_2$ (3.58 g, 20.0 mmol) was added. The reaction mixture was allowed to reach room temperature overnight, the solvents were evaporated under reduced pressure and the resulting orange oil was dried under vacuum at 60 °C (Yield: 4.02 g, 13.6 mmol, 68%). ^{1}H NMR (300 MHz, $CDCl_3$): δ ABX spin system (A = B = H, X = P) 3.24 (2H, dd, J_{AB} = 13.3 Hz, $^2J_{XB}$ = 1.8 Hz), 3.31 (2H, d, J_{AB} = 13.3 Hz), 6.93–6.89 (4H, m, aromatic H), 7.15–7.22 (3H, m, aromatic H), 7.30–7.39 (4H, m, aromatic H), 8.33–8.35 (2H, m, aromatic H); ^{13}C{^{1}H} NMR (75.5 MHz, $CDCl_3$): δ 37.65 (d, $^1J_{PC}$ = 18.4 Hz, P-CH_2), 120.8 (s, CH of pyridyl), 123.6 (d, $^3J_{PC}$ = 5.1 Hz, CH of pyridyl), 128.25 (d, $^3J_{PC}$ = 6.9 Hz, *m*-CH of aryl), 129.1 (s, *p*-CH of aryl), 132.6 (d, $^2J_{PC}$ = 19.9 Hz, *o*-CH of aryl), 136.0 (s, CH of pyridyl), 136.7 (d, $^1J_{PC}$ = 18.4 Hz, C-P of aryl), 149.15 (s, CH of pyridyl), 158.1 (d, $^2J_{PC}$ = 5.7 Hz, N*C*-CH_2 of pyridyl); ^{31}P{^{1}H} NMR (121.5 MHz, $CDCl_3$): δ −12.55. HRMS : Mass calcd for $C_{18}H_{18}N_2P$: 293.1208. Found. 293.1247 [(N,P,N) + H]$^+$.

Synthesis of bis(2-picolyloxy)phenylphosphine 4. Liquid (pyridin-2-yl)methanol (1.39 g, 12.7 mmol) was dissolved in 30 mL of THF and cooled at −78 °C. *n*-BuLi (1 equiv., 12.7 mmol in 8 mL of hexane) was added dropwise and the solution was stirred for 1 h. Then 0.5 equiv. of $PPhCl_2$ (1.15 g, 6.35 mmol) was added dropwise at −78 °C and the mixture was stirred overnight to room temperature. The solvents were removed under reduced pressure and 20 mL of a mixture diethyl ether–CH_2Cl_2 was added to precipitate LiCl. The yellow solution was filtered with a cannula and the solvents were removed under reduced pressure. The resulting yellow oil was dried under vacuum at 60 °C overnight (Yield: 1.75 g, 5.4 mmol, 86%). ^{1}H NMR (300 MHz, $CDCl_3$): δ ABX spin system (A = B = H, X = P) 4.90 (2H, dd, J_{AB} = 13.8 Hz, $^2J_{XB}$ = 7.2 Hz), 5.07 (2H, dd, J_{AB} = 13.8 Hz, $^2J_{XA}$ = 8.4 Hz), 7.15–7.17 (2H, m, aromatic H), 7.44–7.46 (5H, m, aromatic H), 7.62–7.67 (2H, m, aromatic H), 7.71–7.76 (2H, m, aromatic H) 8.50–8.52 (2H, m, CHCN); ^{13}C{^{1}H} NMR (75.5 MHz, $CDCl_3$): δ 69.3 (d, $^2J_{PC}$ = 9.7 Hz, OCH_2), 121.1 (s, CH of pyridyl), 122.4 (s, CH of pyridyl), 128.45 (d, $^3J_{PC}$ = 5.5 Hz, *m*-CH of aryl), 129.8 (s, *p*-CH of aryl), 130.2 (d, $^2J_{PC}$ = 23.9 Hz, *o*-CH of aryl), 136.7 (s, CH of pyridyl), 140.15 (d, $^1J_{PC}$ = 19.6 Hz, P-C of aryl), 149.1 (s, CH of pyridyl), 158.4 (d, $^2J_{PC}$ = 5.4 Hz, N*C*-CH_2 of pyridyl); ^{31}P{^{1}H} NMR (121.5 MHz, $CDCl_3$): δ 161.91.

Synthesis of (pyridin-2-yl)methyl hydrogen phenylphosphonate 5. To a THF solution of (pyridin-2-yl)methanol (3.21 g, 29.4 mmol) containing 10 mL of NEt_3 was added $PPhCl_2$ (2.64 g, 14.7 mmol) at −78 °C. The mixture was stirred overnight at room temperature. All volatiles were removed under reduced pressure and the residue was dissolved in diethyl ether. The solution was filtered and the solvent was removed under reduced pressure to yield a yellow oil (Yield: 40% evaluated by ^{1}H NMR monitoring of the chemical shifts of the CH_2 protons of **4** and **5**). ^{1}H NMR (300 MHz, $CDCl_3$): δ ABX spin system (A = B = H, X = P) 5.16 (1H, dd, J_{AB} = 13.0 Hz, $^2J_{XB}$ = 9.1 Hz), 5.26 (1H, dd, J_{AB} = 13.0 Hz, $^2J_{XA}$ = 9.1 Hz), 7.15–8.51 (9H, m, aromatic H); ^{31}P{^{1}H} NMR (121.5 MHz, $CDCl_3$): δ 27.6 (s).

Synthesis of [Ni{bis(2-picolyl)phenylphosphine}Cl_2] 6. A solution of **1** (1.40 g, 4.8 mmol) in methanol (50 mL) was stirred while $NiCl_2$ (0.62 g, 4.8 mmol) in methanol (50 mL) was added dropwise to the solution. After several hours, the solvent was evaporated and 10 mL of CH_2Cl_2 was added to the red oil. 50 mL of petroleum ether (boiling point 35–60 °C) was added to the solution to precipitate the green complex. After the suspension was sonicated for 1 h, the complex was filtered off and washed several times with diethyl ether. The complex was dried under vacuum (Yield: 2.00 g, 4.6 mmol, 96%). IR (KBr): 1600 (vs), 1566 (m), 1477 (s), 1435 (vs), 1386 (w), 1311 (w), 1155 (m), 1107 (m), 1055 (w), 1016 (w), 820 (w), 745 (s), 694 (m), 482 (m) cm^{-1} (m). Anal. calcd for $C_{18}H_{17}Cl_2N_2NiP$: C, 51.24; H, 4.06; N, 6.64. Found: C, 51.70; H, 4.57; N, 6.32%.

Synthesis of [Ni{bis(4,5-dihydro-2-oxazolylmethyl)phenylphosphine}Cl_2] 7. A solution of **2** (0.90 g, 3.25 mmol) in methanol (50 mL) was stirred while $NiCl_2$ (0.42 g, 3.25 mmol) in methanol (50 mL) was added dropwise to the solution. After several hours the solvent was evaporated and 10 mL of dried and degassed CH_2Cl_2 was added to the red oil. 50 mL of petroleum ether (boiling point 35–60 °C) was added to the solution to precipitate the green complex. After the suspension was sonicated for 1 h, the complex was filtered off and washed several times with diethyl ether. The green complex was dried under vacuum (Yield: 0.80 g, 2.0 mmol, 61%). IR (KBr): 1658 (vs), 1478 (w), 1437 (m), 1402 (s), 1374 (m), 1339 (w), 1270 (s), 1168 (s), 1108 (w), 1034 (s), 999 (w), 972 (w), 932 (m), 868 (w), 749 (m), 694 (m) cm^{-1}. Anal. calcd for $C_{14}H_{17}Cl_2N_2NiO_2P$: C, 41.43; H, 4.22; N, 6.90. Found: C, 40.43; H, 4.42; N, 6.52%.

Synthesis of [Ni{bis(4,4-dimethyl-2-oxazolylmethyl)phenylphosphine}Cl_2] 8. A solution of **3** (2.42 g, 7.3 mmol) in methanol (50 mL) was stirred while $NiCl_2$ (0.94 g, 7.3 mmol) in methanol (50 mL) was added dropwise to the solution. After several hours the solvent was evaporated and 10 mL of dried and degassed CH_2Cl_2 was added to the red oil. 50 mL of petroleum ether (boiling point 35–60 °C) was added to the solution to precipitate the green complex. After the suspension was sonicated for 30 min, the complex was filtered off and washed several times with diethyl ether. Green complex **8** was dried under vacuum (Yield: 2.60 g, 5.6 mmol, 77%). IR (KBr): 1636 (vs), 1464 (m), 1437 (m), 1403 (m), 1369 (s), 1320 (vs), 1162 (s), 1107 (m), 1028 (w), 999 (s), 955 (s), 863 (w), 840 (w), 747 (s), 695 (s) cm^{-1}. Anal. calcd for $C_{18}H_{25}Cl_2N_2NiO_2P$: C, 46.80; H, 5.45; N, 6.06. Found: C, 46.51; H, 5.58; N: 5.77%. Mass calcd for $C_{18}H_{25}ClN_2NiO_2P$: 425.0696. Found. 425.0641 $[Ni(N,P,N)Cl]^+$.

Synthesis of [Ni{bis(2-picolyloxy)phenylphosphine}Cl_2] 9. To a solution of **4** (0.42 g, 1.3 mmol) in CH_2Cl_2 (30 mL) was added $[NiCl_2(DME)]$ (0.30 g, 1.3 mmol). The dark green solution was stirred overnight at room temperature. The solution was concentrated to 5 mL and filtered. 50 mL of petroleum ether was added to the solution to precipitate the complex. After filtration by cannula, the green complex was washed with 20 mL of diethyl ether and dried under vacuum overnight (Yield: 0.51 g, 1.2 mmol, 87%). IR (KBr): 1603 (vs), 1571 (m), 1483 (s), 1463 (s), 1445 (vs), 1385 (w), 1315 (s), 1231 (m), 1164 (m), 1115 (m), 1026 (vs), 995 (vs sh), 836 (s), 800 (s), 770 (s), 734 (s), 713 (m), 691 (m), 626 (s), 548 (s), 485 (m), 431 (m) cm^{-1}. Anal. calcd for $C_{18}H_{17}Cl_2N_2NiO_2P$: C, 47.63; H, 3.77; N, 6.17. Found: C, 47.98; H, 4.21; N, 5.85%. HRMS : Mass calcd for $C_{18}H_{17}ClN_2NiO_2P$: 417.0064. Found. 417.0070 $[Ni(N,P,N)Cl]^+$.

Synthesis of [Fe{bis(2-picolyl)phenylphosphine}$_2$][$Cl_3FeOFeCl_3$] 10. To a solution of **1** (2.40 g, 8.2 mmol) in CH_2Cl_2 (50 mL) was added a CH_2Cl_2 solution of $FeCl_2{\cdot}4H_2O$ (1.63 g, 8.2 mmol) and the mixture was stirred at room temperature overnight. After reaction the brown precipitate was filtered off and washed with diethyl ether. Complex **10** was dried for several hours under vacuum (Yield: 1.70 g, 1.70 mmol, 62%). IR (KBr): 1600 (s), 1471 (vs), 1434 (vs), 1396 (w), 1311 (m), 1155 (m), 1106 (s), 861 (vs), 820 (w), 804 (m), 753 (s), 744 (s sh), 707 (m), 692 (m), 603 (w), 504 (m), 492 (s) cm^{-1}. Anal. calcd for $C_{36}H_{34}Cl_6Fe_3N_4OP_2$: C, 44.08; H, 3.49; N, 5.71. Found: C, 43.96; H, 4.02; N, 6.09%.

Synthesis of [Fe{bis(4,5-dihydro-2-oxazolylmethyl)phenylphosphine}$_2$][$Cl_3FeOFeCl_3$] 11. To a solution of **2** (0.43 g, 1.55 mmol) in CH_2Cl_2 (50 mL) was added a CH_2Cl_2 solution of $FeCl_2{\cdot}4H_2O$ (0.31 g, 1.55 mmol) and the mixture was stirred overnight at room temperature. The violet precipitate was filtered off and washed with diethyl ether. Complex **11** was dried under vacuum (Yield: 0.28 g, 0.3 mmol, 58%). IR (KBr): 1639 (s), 1481 (w), 1435 (w), 1406 (m), 1373 (m), 1269 (vs), 1171 (m), 1108 (w), 999 (w), 933 (m), 858 (w), 745 (m), 694 (m) cm^{-1}. Anal. calcd for $C_{28}H_{34}Cl_6Fe_3N_4O_5P_2$: C, 35.44; H, 3.61; N, 5.91. Found: C, 35.76; H, 4.39; N, 5.98%. HRMS: Mass calcd for $(C_{28}H_{34}FeN_4O_4P_2)/2$: 304.0697. Found: 346.0673 $[Fe(N,P,N)]^{2+}$.

Oligomerization of ethylene

All catalytic reactions were carried out in a magnetically stirred (900 rpm) 145 mL stainless steel autoclave. A 125 mL glass container was used to protect the inner walls of the autoclave from corrosion. The preparation of the catalytic solution of the precatalyst is dependent on the nature and the amount of the cocatalyst.

With $AlEtCl_2$, 4×10^{-2} mmol of Ni complex were dissolved in 14, 13, 12 or 10 mL of cholorobenzene depending on the amount of cocatalyst and injected in the reactor under an ethylene flux. Then 1, 2, 3 or 5 mL of a cocatalyst solution, corresponding to 2, 4, 6 or 10 equiv. respectively, are added to the reactor to achieve a total volume of 15 mL with the precatalyst solution.

With MAO, 4×10^{-2} mmol of Ni complex were dissolved in 10 mL in chlorobenzene and injected into the reactor under an ethylene flux. Then 4, 8 or 16 mL of a cocatalyst solution, corresponding to 100, 200 or 400 equiv. of MAO respectively, were added.

All catalytic tests were started between 25 and 30 °C, and no cooling of the reactor was done during the reaction. After injection of the catalytic solution and of the cocatalyst under a constant low flow of ethylene, the reactor was pressurized to 10 bar. A temperature increase was observed which resulted solely from the exothermicity of the reaction. The 10 bar working pressure was maintained during the experiments through a continuous feed of ethylene from a reserve bottle placed on a balance to allow continuous monitoring of the ethylene uptake. At the end of each test (35 min) a dry ice bath, and in the more exothermic cases also liquid N_2, was used to rapidly cool down the reactor, thus stopping the reaction. When the inner temperature reached 0 °C the ice bath was removed allowing the temperature to slowly rise to 10 °C. The gaseous phase was then transferred into a 10 L polyethylene tank filled with water. An aliquot of this gaseous phase was transferred into a Schlenk flask, previously evacuated, for GC analysis. The products in the reactor were hydrolyzed *in situ* by the addition of ethanol (1 mL), transferred into a Schlenk flask, and separated from the metal complexes by trap-to-trap evaporation (20 °C, 0.8 mbar) into a second Schlenk flask previously immersed in liquid nitrogen in order to avoid any loss of product.

Electrochemical measurements

Electrochemical experiments were performed with a three-electrode system consisting of a platinum working electrode, a platinum-wire counter electrode, and a silver wire as pseudo-reference. The redox potentials are reported *versus* the saturated calomel electrode after correction using ferrocene. All measurements were carried out under Ar, in degassed and distilled MeCN, using 0.1 M $[N(n\text{-}Bu)_4]PF_6$ solutions as the supporting electrolyte. An EG & G Princeton Applied Research Model 273A potentiostat connected to a computer (Programme Research Electrochemistry Software) was used.

Crystal structure determinations

Diffraction data were collected on a Kappa CCD diffractometer using graphite-monochromated Mo-Kα radiation ($\lambda = 0.71073$ Å) (Table 5). Data were collected using phi-scans and the structures were solved by direct methods using the SHELX 97 software,[48,49]

Table 5 X-Ray experimental data for **10**·0.5CH$_2$Cl$_2$ and **11**·4MeCN

Crystal data	**10**·0.5CH$_2$Cl$_2$	**11**·4MeCN
Chemical formula	$C_{36}H_{34}FeN_4P_2\cdot0.5(CH_2Cl_2)\cdot Fe_2OCl_6$	$C_{28}H_{34}FeN_4O_4P_2\cdot4(C_2H_3N)\cdot Fe_2Cl_6O$
M_r	1023.33	1113.00
Crystal system	Orthorhombic	Monoclinic
Space group	*Pccn*	*C*2/*c*
T/K	173(2)	173(2)
a/Å	12.6010(3)	15.3270(7)
b/Å	16.6710(5)	21.8930(12)
c/Å	20.3170(6)	15.4880(9)
β/°	90.00	110.368(2)
V/Å^3	4268.0 (2)	4872.1 (4)
Z	4	4
D_x/Mg m^{-3}	1.593	1.517
Radiation type	Mo $K\alpha$	Mo $K\alpha$
μ/mm^{-1}	1.55	1.32
Crystal form, colour	Prism, orange	Prism, red
Crystal size/mm	0.12 × 0.10 × 0.10	0.14 × 0.12 × 0.10
F(000)	2068	2272
No. of measd, indep. and obsd reflect.	9257, 4894, 3202	12328, 7114, 5370
R_{int}	0.070	0.033
θ_{max}/°	27.5	30.0
$R[F^2 > 2\sigma(F^2)]$, $wR(F^2)$, S	0.088, 0.168, 1.15	0.050, 0.090, 1.06
No. of relections	4894	7114
No. of parameters	247	272

and the refinement was by full-matrix least squares on F^2. No absorption correction was used. All non-hydrogen atoms were refined anisotropically with H atoms introduced as fixed contributors ($d_{\text{C–H}} = 0.95$ Å, $U_{11} = 0.04$).

Acknowledgements

We thank the Centre National de la Recherche Scientifique (CNRS), the Ministère de l'Education Nationale et de la Recherche (Paris) and the Institut Français du Pétrole (IFP) for support. We are grateful to the Erasmus-Socrates exchange programme between the University Duisburg-Essen and ULP (F. T.). We also thank Dr A. DeCian and Prof. R. Welter (ULP Strasbourg) for the crystal structure determinations, Dr Jean-Paul Collin (ULP Strasbourg) for the electrochemical measurements and M. Mermillon-Fournier (LCC Strasbourg) for technical assistance.

References

1 For recent reviews, see: (*a*) G. J. P. Britovsek, V. C. Gibson and D. F. Wass, *Angew. Chem., Int. Ed.*, 1999, **38**, 428; (*b*) S. D. Ittel, L. K. Johnson and M. Brookhart, *Chem. Rev.*, 2000, **100**, 1169; (*c*) *Late Transition Metal Polymerization Catalysis*, ed. B. Rieger, L. Saunders Baugh, S. Kacker and S. Striegler, Wiley-VCH, New York, 2003; (*d*) V. C. Gibson and S. K. Spitzmesser, *Chem. Rev.*, 2003, **103**, 283; (*e*) F. Speiser, P. Braunstein and L. Saussine, *Acc. Chem. Res.*, 2005, **38**, 784; (*f*) C. Bianchini, G. Giambastiani, I. G. Rios, G. Mantovani, A. Meli and A. M. Segarra, *Coord. Chem. Rev.*, 2006, **250**, 1391; (*g*) S. Jie, S. Zhang, K. Wedeking, W. Zhang, H. Ma, X. Lu, Y. Deng and W.-H. Sun, *C. R. Chim.*, 2006, **9**, 1500.

2 A. Kermagoret and P. Braunstein, *Organometallics*, 2008, **27**, 88.

3 F. Speiser, P. Braunstein and L. Saussine, *Dalton Trans.*, 2004, 1539.

4 A. Kermagoret and P. Braunstein, *Dalton Trans.*, 2008, 585.

5 P. Braunstein, F. Naud, A. Dedieu, M.-M. Rohmer, A. DeCian and S. J. Rettig, *Organometallics*, 2001, **20**, 2966.

6 D. Fenske, B. Maczek and K. Maczek, *Z. Anorg. Allg. Chem.*, 1997, **623**, 1113.

7 E. Lindner, H. Rauleder and W. Hiller, *Z. Naturforsch., B: Anorg. Chem. Org. Chem.*, 1983, **38**, 417.

8 P. Braunstein, M. D. Fryzuk, F. Naud and S. J. Rettig, *J. Chem. Soc., Dalton Trans.*, 1999, 589.

9 O. Kühl, P. C. Junk and E. Hey-Hawkins, *Z. Anorg. Allg. Chem.*, 2000, **626**, 1591.

10 (*a*) L. M. Venanzi, *J. Chem. Soc. A*, 1958, 719; (*b*) D. F. Evans, *J. Chem. Soc. A*, 1959, 2003.

11 J. L. Deutsch and S. M. Poling, *J. Chem. Educ.*, 1969, **46**, 167.

12 J. Löliger and R. Scheffold, *J. Chem. Educ.*, 1972, **49**, 646.

13 S. K. Sur, *J. Magn. Reson.*, 1989, **82**, 169.

14 F. Speiser, P. Braunstein, L. Saussine and R. Welter, *Inorg. Chem.*, 2004, **43**, 1649.

15 F. Speiser, P. Braunstein, L. Saussine and R. Welter, *Organometallics*, 2004, **23**, 2613.

16 F. Speiser, P. Braunstein and L. Saussine, *Organometallics*, 2004, **23**, 2633.

17 A. Kermagoret, R. Pattacini, P. C. Vasquez, G. Rogez, R. Welter and P. Braunstein, *Angew. Chem., Int. Ed.*, 2007, **46**, 6438.

18 P. Braunstein, F. Naud, A. Pfaltz and S. J. Rettig, *Organometallics*, 2000, **19**, 2676.

19 S. Ameerunisha, J. Schneider, T. Meyer, P. S. Zacharias, E. Bill and G. Henkel, *Chem. Commun.*, 2000, 2155.

20 B. C. Childs and H. A. Goodwin, *Aust. J. Chem.*, 2001, **54**, 685.

21 Y. Chen, C. Qian and J. Sun, *Organometallics*, 2003, **22**, 1231.

22 (*a*) A. Machkour, D. Mandon, M. Lachkar and R. Welter, *Inorg. Chem.*, 2004, **43**, 1545; (*b*) F. Li, M. Wang, C. Ma, A. Gao, H. Chen and L. Sun, *Dalton Trans.*, 2006, 2427–2434.

23 L. P. Wu, Y. Yamagiwa, I. Ino, K. Sugimoto, T. Kuroda-Sowa, T. Kamikawa and M. Munakata, *Polyhedron*, 1999, **18**, 2047.

24 Y. Nakayama, Y. Baba, H. Yasuda, K. Kawakita and N. Ueyama, *Macromolecules*, 2003, **36**, 7953.

25 F. Pelascini, M. Wesolek, F. Peruch, A. De Cian, N. Kyritsakas, P. J. Lutz and J. Kress, *Polyhedron*, 2004, **23**, 3193.

26 A. S. Ionkin, W. J. Marshall, D. J. Adelman, B. Bobik Fones, B. M. Fish and M. F. Schiffhauer, *Organometallics*, 2006, **25**, 2978.

27 A. A. Danopoulos, N. Tsoureas, J. A. Wright and M. E. Light, *Organometallics*, 2004, **23**, 166.

28 M. G. B. Drew, V. McKee and S. M. Nelson, *J. Chem. Soc., Dalton Trans.*, 1978, 80.

29 P. C. Healy, B. W. Skelton and A. H. White, *Aust. J. Chem.*, 1983, **36**, 2057.

30 M. James, H. Kawaguchi and K. Tatsumi, *Polyhedron*, 1997, **16**, 4279.

31 D. B. Dell'amico, F. Calderazzo, L. Labella, F. Marchetti and E. G. F. Quadrelli, *Gazz. Chim. Ital.*, 1997, **127**, 103.

32 K. R. Dunbar, J. J. Longridge, J. M. Rawson, J.-S. Sun, K. S. Hagen and B. Do, *Inorg. Synth.*, 2002, **33**, 103.
33 W. M. Reiff, E. H. Witten, K. Mottle, T. F. Brennan and A. R. Garafalo, *Inorg. Chim. Acta*, 1983, **77**, L83.
34 H. Weiss and J. Strähle, *Z. Naturforsch., B: Anorg. Chem. Org. Chem.*, 1984, **39**, 1453.
35 N. Kuhn, H. Kotowski, C. Maichle-Moessmer and U. Abram, *Z. Anorg. Allg. Chem.*, 1998, **624**, 1653.
36 M. Bolte, H. W. Lerner and S. Scholz, *Acta Crystallogr., Sect. E: Struct. Rep. Online*, 2001, **57**, m216.
37 G. J. P. Britovsek, V. C. Gibson, S. K. Spitzmesser, K. P. Tellmann, A. J. P. White and D. J. Williams, *J. Chem. Soc., Dalton Trans.*, 2002, 1159.
38 K. P. Tellmann, V. C. Gibson, A. J. P. White and D. J. Williams, *Organometallics*, 2005, **24**, 280.
39 P. Braunstein and F. Naud, *Angew. Chem., Int. Ed.*, 2001, **40**, 680.
40 P. S. Braterman, J. I. Song and R. D. Peacock, *Inorg. Chem.*, 1992, **31**, 555.
41 A. Cabort, A. Michel, B. Therrien, H. Stoeckli-Evans, K. Bernauer, G. Suss-Fink, A. F. Williams and G. Stupka, *Inorg. Chim. Acta*, 2003, **350**, 193.
42 V. C. Gibson, R. K. O'Reilly, W. Reed, D. F. Wass, A. J. P. White and D. J. Williams, *Chem. Commun.*, 2002, 1850.
43 N. Bergem, U. Blindheim, O. T. Onsager and H. Wang, *Fr. Pat.*, Fr 1 519 181, 1968.
44 L. P. Spencer, R. Altwer, P. Wei, L. Gelmini, J. Gauld and D. W. Stephan, *Organometallics*, 2003, **22**, 3841.
45 W.-H. Sun, X. Tang, T. Gao, B. Wu, W. Zhang and H. Ma, *Organometallics*, 2004, **23**, 5037.
46 D. M. Dawson, D. A. Walker, M. Thornton-Pett and M. Bochmann, *J. Chem. Soc., Dalton Trans.*, 2000, 459.
47 D. S. McGuinness, V. C. Gibson and J. W. Steed, *Organometallics*, 2004, **23**, 6288.
48 *Kappa CCD Operation Manual*, Nonius BV, Delft, The Netherlands, 1997.
49 G. M. Sheldrick, *SHELXL97, Program for the refinement of crystal structures*, University of Göttingen, Germany, 1997.